IEEE Access
Multidisciplinary | Rapid Review | Open Access Journal

Received 9 June 2024, accepted 21 July 2024, date of publication 30 July 2024, date of current version 26 August 2024.

Digital Object Identifier 10.1109/ACCESS.2024.3435768

RESEARCH ARTICLE

LEADNet: Detection of Alzheimer's Disease Using Spatiotemporal EEG Analysis and Low-Complexity CNN

DIGAMBAR V. PURI[1], PRAMOD H. KACHARE[1], SANDEEP B. SANGLE[1], RAIMUND KIRNER[2], ABDOH JABBARI[3], IBRAHIM AL-SHOURBAJI[2,3], MOHAMMED ABDALRAHEEM[4], AND ABDALLA ALAMEEN[5]

[1]Department of Computer Science and Engineering, Ramrao Adik Institute of Technology, D. Y. Patil Deemed to be University, Navi Mumbai 400706, India
[2]Department of Computer Science, University of Hertfordshire, AL10 9AB Hatfield, U.K.
[3]Department of Electrical and Electronics Engineering, Jazan University, Jazan 45142, Saudi Arabia
[4]Department of Computer Science, Jazan University, Jazan 45142, Saudi Arabia
[5]Department of Computer Engineering and Information, Prince Sattam Bin Abdulaziz University, Wadi ad-Dawasir 11991, Saudi Arabia

Corresponding authors: Ibrahim Al-Shourbaji (alshourbajiibrahim@gmail.com) and Raimund Kirner (r.kirner@herts.ac.uk)

The article processing charge for this article has been funded by the University of Hertfordshire.

ABSTRACT Clinical methods for dementia detection are expensive and prone to human errors. Despite various computer-aided methods using electroencephalography (EEG) signals and artificial intelligence, a reliable detection of Alzheimer's disease (AD) remains a challenge. The existing EEG-based machine learning models have limited performance or high computation complexity. Hence, there is a need for an optimal deep learning model for the detection of AD. This paper proposes a low-complexity EEG-based AD detection CNN called LEADNet to generate disease-specific features. LEADNet employs spatiotemporal EEG signals as input, two convolution layers for feature generation, a max-pooling layer for asymmetric spatiotemporal redundancy reduction, two fully-connected layers for nonlinear feature transformation and selection, and a softmax layer for disease probability prediction. Different quantitative measures are calculated using an open-source AD dataset to compare LEADNet and four pre-trained CNN models. The results show that the lightweight architecture of LEADNet has at least a 150-fold reduction in network parameters and the highest testing accuracy of 99.24% compared to pre-trained models. The investigation of individual layers of LEADNet showed successive improvements in feature transformation and selection for detecting AD subjects. A comparison with the state-of-the-art AD detection models showed that the highest accuracy, sensitivity, and specificity were achieved by the LEADNet model.

INDEX TERMS Alzheimer's disease, convolutional neural network, electroencephalogram, pre-trained models.

I. INTRODUCTION

The most prevalent form of dementia that targets older adults is Alzheimer's disease (AD). Cognitive dysfunctions, trouble with daily tasks, aphasia, impaired judgment, and diminished memory are some of the characteristics of AD [1]. AD cannot be cured, but its incidence can decrease with prompt detection. An early phase of AD known as mild cognitive impairment (MCI) affects 5-20% of older persons (age over 60) [2]. Most MCI sufferers are mainly unaware of the signs as they go about their regular lives. Since AD symptoms sometimes coincide with those of aging, it is challenging to recognize the disease early at the MCI stage. The number of individuals suffering from AD will rise from 60 million in 2020 to over 130 million in 2050, as confirmed by the work of the Alzheimer's Association [3]. Also, compared to wealthy nations, the incidence of AD is much greater in developing countries.

The associate editor coordinating the review of this manuscript and approving it for publication was Nuno M. Garcia.

Since there is currently no treatment for AD, medicines can postpone the disease's severe stages [4]. Thus, it is imperative to have a computerized AD detection system in the initial stages. Early detection and appropriate safeguards can help people with AD retain their autonomy for longer while reducing social expenses and despair [5]. Numerous neurological, biochemical, and psychosocial tests are used to diagnose AD. The clinical diagnosis is an arbitrary process that relies on a neurologist's skill [6], [7]. AD is diagnosed using a variety of neuroimaging techniques, including positron emission tomography (PET), single-photon emission computed tomography (SPECT), and magnetic resonance imaging (MRI). Still, imaging-based methods for detecting AD are expensive, laborious, and subject to high radiation [8]. The Electroencephalogram (EEG) has gained recognition for identifying neurological disorders seen in individuals with AD, thereby overcoming the constraints of conventional approaches. EEG-based systems can be implemented at a low cost, with non-invasive features, high temporal resolution, and sensitivity [9]. Compared to normal controlled (NC) people, AD patients exhibit more EEG slowdown, decreased synchronization, and reduced signal diversity [10]. Literature reports several binary classes as AD vs. MCI, AD vs. NC, or MCI vs. NC.

Approaches, such as Shannon entropy (ShEn) [11], sample entropy (SampEn) [12], approximate entropy (ApEn), epoch-based entropy, spectral entropy (SpEn) [13], wavelet entropy, Tsallis entropy [14], auto mutual information (MI) [15], Kolmogorov complexity [16], multiscale entropy (MSEn) [17], permutation entropy (PrEn), sure entropy (SuEn), fuzzy entropy (FuEn) [18], Hjorth parameters [19], β/θ entropy ratio [20], and Lempel Ziv complexity (LZC) [21] have been investigated. However, the signal length and different input parameters primarily affect ApEn, SampEn, MSEn, and LZC values. Dauwels et al. [22] investigated the comparative study of various synchrony measures for early diagnosis of AD patients. These metrics include Granger causality (GC), phase synchrony, association entropy, synchronization entropy, probabilistic occurrence harmony, information-theoretic metrics, and synchronization function. According to the studies in [22], GC and stochastic events are the most effective ways to differentiate between AD and NC patients. The studies relied on the time domain characteristics before obtaining substantial frequency data. Cataldo et al. [23] investigated the multiscale FuEn to detect the AD. They concluded that AD subjects displayed higher complexity values for low-frequency bands than NC subjects, while the opposite was found in fast-frequency bands. Criscuolo et al. [24] extended the work using MFE with magnitude-square coherence and obtained 93.50% accuracy. It has been noted that the majority of research in recent years included wavelet decomposition, nonlinear algorithms, Fast Fourier Transform (FFT), and empirical mode decomposition (EMD) in conjunction with window choice, sequence of filters, and wavelets to identify AD. Because EEG signals are unpredictable, choosing breakdown values for EMD, discrete wavelet transform, and variational mode decomposition is laborious. Nonlinear methods are dependent on parameters, such as entropy-based methods. As a result, choosing the essential factors is complex. Furthermore, signal analysis, feature extraction, and categorization are time-consuming. Research abundantly shows that the custom characteristics have a dynamic categorization rate. Furthermore, these require extensive statistical evaluation, both qualitative and quantitative, which impacts the precision of the system. A deep neural network (DNN) model is a classifier and feature generator hybrid. As a result, the process of computing and choosing features is automated.

A computerized identification of AD framework based on DNN and EEG signals is presented to address these problems. The less complex AD detection convolution neural network (LEADNet) has been designed to lower the computational burden while maintaining a high AD detection rate. Additionally, the variable feature correlation technique was used to reduce the number of variables trained in the convolutional neural network (CNN) to determine the computing overhead to ensure only features with strong correlations are considered. At first, all EEG readings underwent pre-processing to eliminate the 60 Hz powerline frequency. A 40th-order Chebyshev filters remove the noise, and the CNN and other learned deep-learning models, such as VGG16, VGG19, ResNet50, and EfficientNetB4, are fed filtered AD and NC EEG signals. A summary of paper contributions is as follows:

- Improving the automatic AD detection model by utilizing spatiotemporal EEG analysis and introducing a simpler CNN-based, the LEADNet, to reduce computation delay.
- Extracting AD-specific nonlinear features using convolutional layers, minimizing redundancyusing a max-pooling layer, identifying salient feature susing fully-connected layers, and estiamting likelihood of AD using softmax layer.
- Evaluating LEADNet's classification performance and computational complexity against existing AD detection techniques and pre-trained models.
- Discriminating between AD and NC EEG recordings and presenting generalization by visualizing the layers of the LEADNet model

The rest of the paper is structured as follows. Section II describes the proposed methodology. In section III, the experimental results are discussed. Section IV compares the planned work and the most advanced techniques. Section 5 provides the conclusions.

II. PROPOSED METHOD

Deep neural networks (DNN) are considered to assess the significance of EEG signals in identifying AD. The flow of the EEG dataset and classification algorithms is provided below. The autoamtic AD detection process flow is depicted in Fig. 1 followed by a comprehensive explanation of the method.

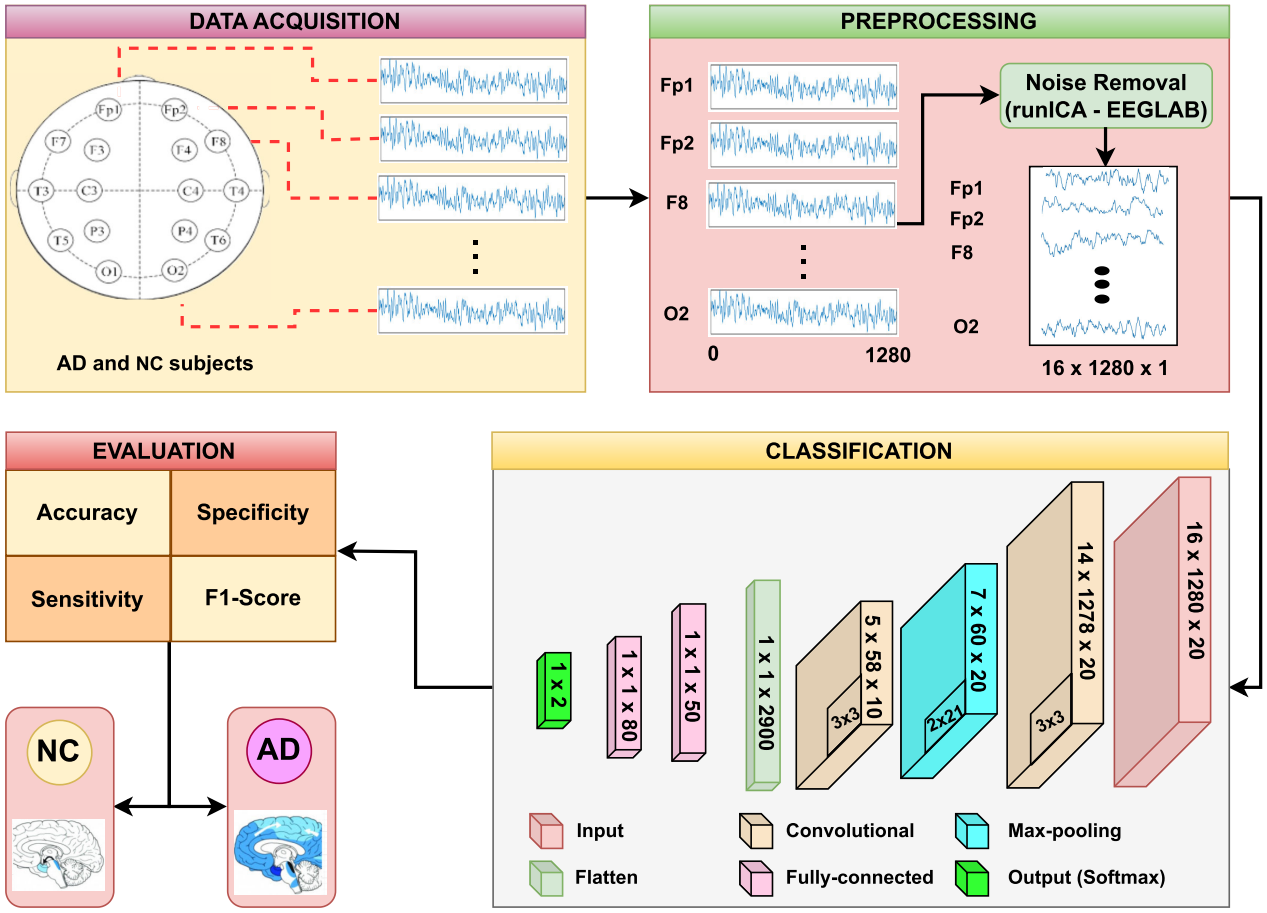

FIGURE 1. Schematic of the proposed LEADNet-based Alzheimer's detections system.

A. EEG DATASET

The EEG signals from 11 NC subjects (4 male & 7 female) and 12 AD patients (5 male & 7 female) make up the dataset [25]. Every AD patient belonged to the Valladolid Alzheimer's Individuals Family Organisation (AFAVA). Participants were screened for the existence of undesirable neurological conditions, such as epilepsy, Parkinson's disease, etc., throughout the hiring procedure. The MMSE average for individuals with AD was 13.1, with a 5.9 standard deviation. The MMSE scores of NC participants were higher than 30 [26]. Each subject's EEG signals were captured for five seconds using the 2.3.411 EEG profile study room equipment from Oxford Instruments. The 12-bit analog-to-digital conversion is used to digitise the EEG data at a rate of sampling of 256 Hz. Table 1 lists the characteristics of the EEG signals for both AD and NC subjects.

This work uses a 40th-order Chebyshev broadband filter of 0.5-100Hz to eliminate the frequencies above 100Hz and the DC line. After that, we used a notch filter with a 60Hz. Data segments that are longer than 1 sec are removed. Additionally, the ICA (*RunICA* from EEGLAB) is used to implement the Independent Component Analysis (ICA) approach. ICA technique that can decompose these mixed signals into independent components, making it possible to identify and isolate noise sources. This processing created 16 unique ICA components from the original 16-channel EEG signals. The automatic classification tool ICLabel on the EEGLAB platform was used in the procedure to identify eye or jaw artifacts from particular ICA components. The EEG signals of these detected artifact components were cleaned.

TABLE 1. EEG dataset details used in this work.

Parameters	AD patients	NC subjects
No. of signals	400	263
Signal duration	5 sec (1280 Samples)	5 sec (1280 Samples)
No. of subjects	12	11
Sampling Frequency	256 Hz	256 Hz
Samples per signal	1280×16=20480	1280×16=20480
Age	72.8±8 years	72.5±6.1 years
No. of trials	34	24

B. FEATURE EXTRACTION

The techniques used for feature extraction are described in this section. Convolutional neural networks (CNN) with a

TABLE 2. Architectural of the proposed LEADNet model.

Layer type	Layer output	Parameters
Input	(16, 1280, 1)	
Conv2D	(14, 1278, 20)	200
MaxPooling2D	(7, 60, 20)	0
Conv2D	(5, 58, 10)	1810
Flatten	(2900)	0
Fully Connected-1	(50)	145050
Fully Connected-2	(80)	4080
Softmax	(2)	162
Trainable parameters		1,51,302

max-pooling layer are used for feature extraction. Following these techniques, the recovered parameters for the AD and NC EEG signals are passed via thick and flattened layers. The last layer categorizes the features that the preceding three layers have extracted. The LEADNet architecture is detailed in Table 2, along with each layer's trainable parameters and output dimension. Each block of LEADNet comprises a 2D convolutional layer to learn feature maps using suitable weights. As shown in Fig. 1, input data of EEG signal with the shape of (16, 1280) applied to LEADNet. Here, 16 and 1280 are the frequency and duration of the EEG signal samples. The input EEG signal is combined with 20 kernels, each measuring 3 × 3, in the first layer of the LEADNet to produce an outcome shape of (14, 1278, 20). These make the number of trainable parameters 200. The max-pooling layer selects the highest level patterns in the input EEG signals. It is achieved by enhancing the span of convolutional calculation [27] using the following calculation:

$$y_{max}(h, v) = max(\{x(h + s, v + s); 0 \leq h < H, 0 \leq h < V\}) \tag{1}$$

where H is horizontal kernel size, V is vertical kernel sizes, and s is a stride. A 2×21 kernel is selected to extract max values from 14×1280 input features in the max pooling layer.

A larger kernel size in the max-pooling layer can capture more temporal information from the input features. This kernel size helps to reduce the redundancy and extract the most essential features for further processing. After max-pooling, the feature map shape becomes (7, 60, 20). This layer does not introduce any additional parameters. The second 2D convolutional layer exposes 2,900 trainable parameters and generates an output shape of (5, 58, 10). The classifier converts the feature extraction stage's output into a vector. At this point, dropout and fully connected layers are utilized instead of convolution and max-pooling layers. In the fully-connected layer, there are between 50 and 80 neurons.

Due to fewer neurons, the computation complexity for dense layers decreases linearly with fewer variables that can be trained. For each output label, a probabilistic score is produced by a softmax layer. The network weights are trained using the Adam optimizer that integrates stochastic root mean square propagation and stochastic gradient descent. The Adam optimizes the learning rate in the network. In addition, its accuracy is superior to that of the SGD and RMSP optimization methods.

For k^{th} predicted probability of m^{th} training example $\{y_{predic}(l, k) | s.t. \sum_k y_{predic}(l, k) = 1, \forall l\}$. The cross-entropy loss is calculated as:

$$\text{Crossentropy Loss} = -\sum_{l-1}^{N_{train}} \sum_{k-1}^{N_{class}} y(l, k) \times \log y_{predic}(l, k) \tag{2}$$

where N_{train} and N_{class} are the total number of training samples and number of classes, respectively. As shown in Fig. 1, the trainable parameters from dense and convolution layers are minimized in the proposed LEADNet.

1) EVALUATION METRICS

The effectiveness of ML classifiers is assessed using different parameters such as accuracy (CA), sensitivity (SNS), specificity (SPC), and F1-score (F1) [28], [29]. These parameters are calculated as:

$$CA = \frac{Ta + Tn}{Ta + Tn + Fa + Fn} \times 100 \tag{3}$$

$$SNS = \frac{Ta}{Ta + Fn} \times 100 \tag{4}$$

$$SPC = \frac{Tn}{Tn + Fa} \times 100 \tag{5}$$

$$F1 = \frac{2 \times Ta}{2 \times Ta + Fa + Fn} \times 100 \tag{6}$$

$$MACC = \frac{Tn \times Ta - Fn \times Fa}{\sqrt{(Ta + Fa)(Ta + Fn)(Tn + Fa)(Tn + Fn)}} \times 100 \tag{7}$$

$$G - mean = \sqrt{SNS \times SPC} \tag{8}$$

Here, Ta and Tn are AD and NC subjects detected correctly, respectively. Fn is AD patients detected as NC (falsely AD) and Fa is NC subjects detected as AD (falsely NC) [30].

Algorithm 1 LEADNet Training Process

```
Input: Labelled Spatiotemporal EEG data
Output: Trained LEADNet model
Split data training-validation-testing (70-10-20 %)
Initialize LEADNet architecture
Initialize hyperparameters of LEADNet
while epoch < max_epoch do
    while batch < max_batch do
        Generate LEADNet outputs for training data
        Estimate validation outputs & compute loss
        Compute gradients using training data
        Update LEADNet parameters using gradients
    end while
end while
Evaluate performance using testing data
```

TABLE 3. Performance evaluation using LEADNet and other pre-trained CNNs.

Model	Dataset	CA	SNS	SPC	F1	MCC	κ-value	G-mean
VGG16	Training	94.55	94.59	94.56	94.58	94.98	92.45	94.58
	Validation	92.45	92.52	92.45	92.48	81.13	91.89	92.48
	Testing	96.24	95.00	98.11	96.82	91.64	90.82	95.66
VGG19	Training	94.97	95.34	95.28	95.31	95.35	94.65	95.30
	Validation	98.11	98.19	98.11	98.15	88.68	88.75	98.14
	Testing	96.99	97.48	96.43	97.45	91.65	90.84	95.67
ResNet50	Training	99.24	98.97	98.97	98.97	99.58	98.55	98.97
	Validation	96.23	96.35	96.23	96.40	92.45	94.97	96.28
	Testing	96.99	98.67	94.83	98.02	99.30	94.03	97.10
EfficiantNet-B4	Training	82.18	82.19	82.19	82.19	66.04	83.45	82.19
	Validation	84.91	84.95	84.92	84.93	66.01	84.56	84.93
	Testing	88.72	90.80	93.48	93.49	93.49	79.55	92.13
LEADNet	Training	100	100	99.84	99.89	100	100	99.91
	Validation	99.06	99.26	99.15	99.33	99.24	97.45	99.37
	Testing	99.24	100	98.18	99.35	98.45	98.41	99.08

III. RESULTS AND DISCUSSION

This section uses various pre-trained models, including VGG16, VGG19, ResNet50, and EfficientNetB4 for comparison purposes. To ensure the robustness of our performance evaluation and prevent data leakage, we used a train, test, and validation data splitting method. Here, 70% of the data is used for training the model. 10% of the data is used for model validation and hyperparameter tuning, and 20% for testing the model. Table 4 shows the confusion matrix of LEADNet on the testing dataset. The confusion matrix shows the classification results of the model, where the *Ta* rate is high, and the *Fa* and *Fn* rates are low. The hyperparameters of the proposed LEADNet and the state-of-the-art pre-trained networks are presented in Table 5.

A. COMPARISON WITH PRE-TRAINED MODELS

Table 3 compares different pre-trained and suggested LEADNet performance metrics in terms of CA, SNS, SPC, and F1-score. The LEADNet has 99.24% CA, 100% SNS, 98.18% SPC, 99.35% F1-score, MCC 98.45%, Kappa 98.41%, and the geometric mean 99.08% in the testing stage.

TABLE 4. Confusion matrix of LEADNet models.

	Predicted Positive	Predicted Negative
Actual Positive	76	1
Actual Negative	1	55

The VGG19 also performed better than VGG16, ResNet50, and EfficiantNet-B4, with a testing accuracy of 96.99%. The more pre-trained parameters in EfficiantNet-B4 caused the worst training, validation, and testing performance.

In the comparison of models, the learning rate is set to 0.0001 for LEADNet, VGG16, and EfficientNetB4, while it is set to 0.001 for the other models. Additionally, all models are trained for 150 epochs, maintaining consistency across the experiments. In contrast, this part uses multiple pre-trained models, such as VGG16, VGG19, ResNet50, and EfficientNetB4. Table 5 presents the hyperparameters of the state-of-the-art pre-trained networks and the proposed LEADNet. The learning rate for LEADNet, VGG16, and EfficientNetB4 in the model comparison is 0.0001, but it is set to 0.001 for the other models. Furthermore, all models undergo 150 training epochs to ensure uniformity throughout the studies.

TABLE 5. Hyper-parameter setting for different models.

Model	Batch size	Epoch	Total Parameters
VGG16	120	110	1,47,44,580
VGG19	110	100	2,00,54,276
ResNet50	80	100	23,694,404
EfficiantNet-B4	80	100	1,77,67,715
LEADNet	80	50	1,51,302

The convergence analysis has been performed on all models, including the proposed LEADNet. From the convergence analysis, the stability of learning patterns can be learned over many epochs. Figures 2-6 depict all the model's accuracy and loss plots over the number of epochs. These accuracy and loss curves show the convergence over time as the model learns from the data. This convergence indicates that the model is improving and approaching an optimal solution. The accuracy and loss curves of VGG-16 and ResNet50, Figures 2 and 4, indicate the dissimilarities between all training and validation curve epochs compared to other models' accuracy and loss curves. Similarly, for the VGG-19 and the LEADNet, Figures 3 and 6 show the difference between 0 to 25 epochs and 5 to 15 epochs, respectively. The accuracy and loss curve of the EfficientNetB4 is continuously fluctuating. This fluctuation can occur due to the stochastic nature of specific algorithms.

B. VISUALIZATION OF LEADNET LAYERS

The flattened layer data distribution plots of VGG16, VGG19, ResNet50, EfficientNetB4, and LEADNet are

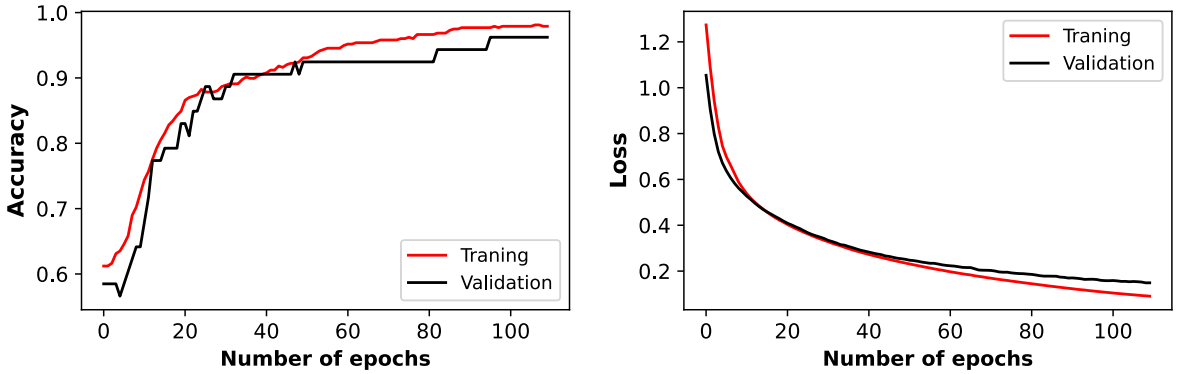

FIGURE 2. Training and validation accuracy (left) and loss (right) curves using VGG16.

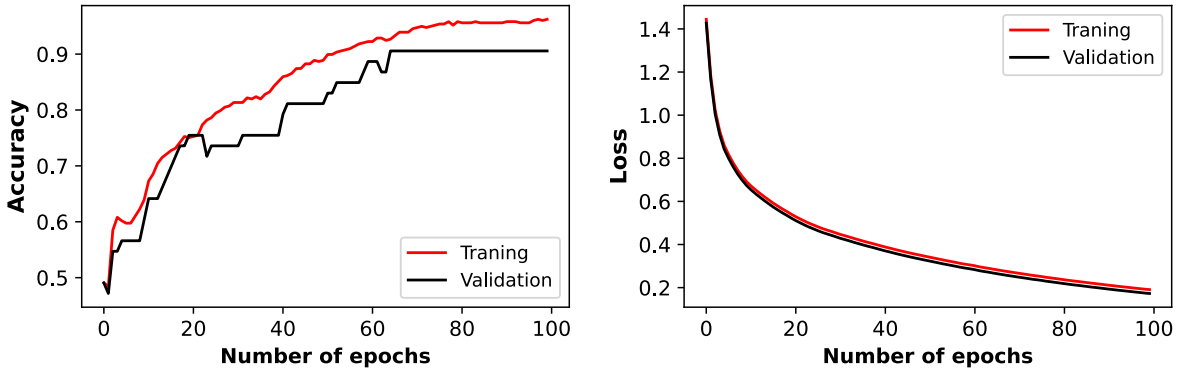

FIGURE 3. Training and validation accuracy (left) and loss (right) curves using VGG19.

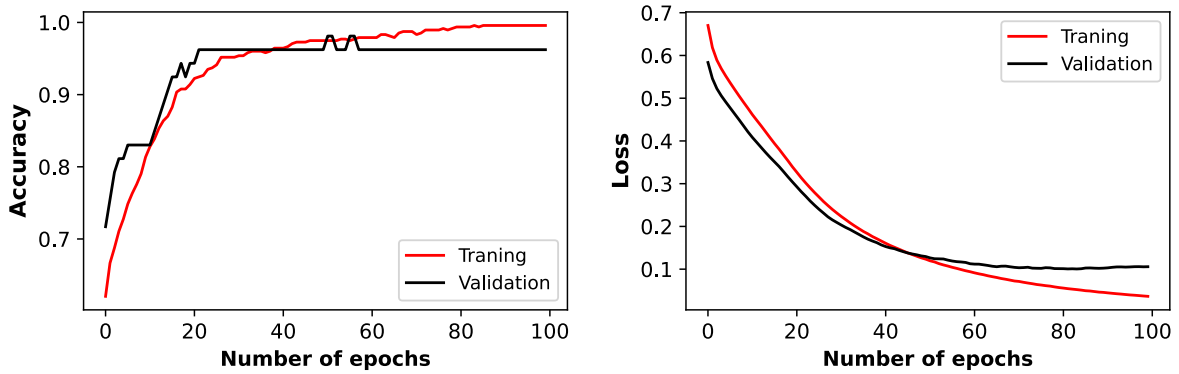

FIGURE 4. Training and validation accuracy (left) and loss (right) curves using ResNet50.

depicted in Fig. 7. The flattened layer is used to transform multi-dimensional data into a one-dimensional array. This operation is typically applied before feeding the data into a fully connected layer, which requires one-dimensional input. So, the flattened layer plays a vital role in the model to observe the model's behavior and complexity. The flattened layer data is distributed using the t-distributed stochastic 160 neighbor embedding (t-SNE) for visualizing data. This data distribution shows both class samples with different colors. The complexity of the model can be observed through that distribution plot. Except for the EfficientNetB4, all the models of the distribution plots can be separated easily. The feature maps revealed altered patterns for AD compared to NC EEG recordings, indicating potential biomarkers and neurophysiological changes.

In summary, these feature maps emphasize the important input data regions for detection and become more informative for deeper layers. The results underscore the potential of the LEADNet model to distinguish AD and NC EEG recordings. The visualizations of feature maps aids to develope quantitative and objective methods for detection and monitoring of the Alzheimer's disease.

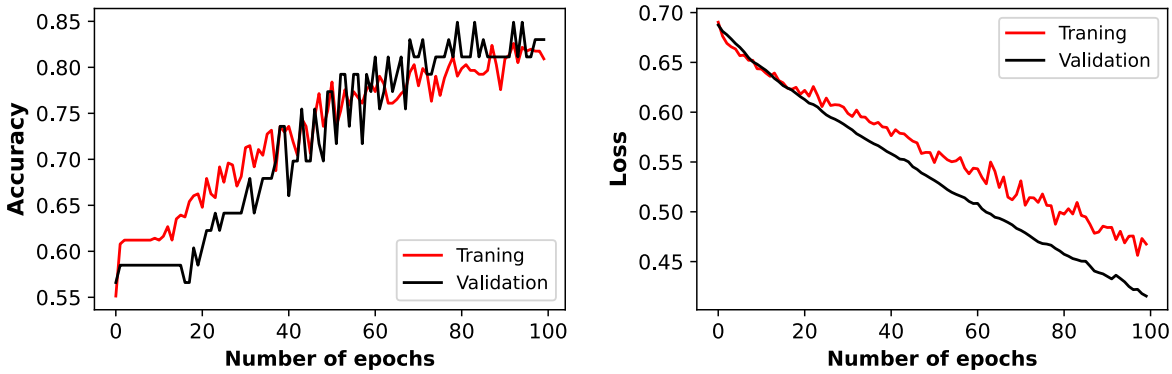

FIGURE 5. Training and validation accuracy (left) and loss (right) curves using EfficientNetB4.

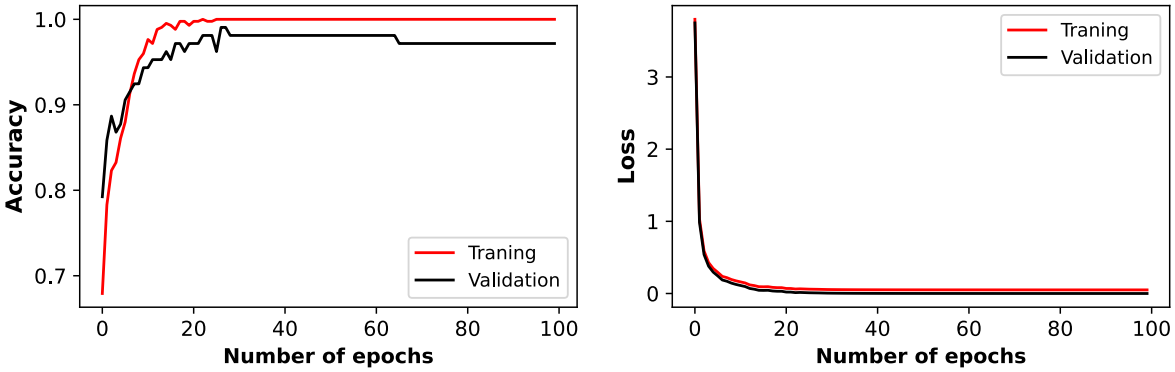

FIGURE 6. Training and validation accuracy (left) and loss (right) curves using LEADNet.

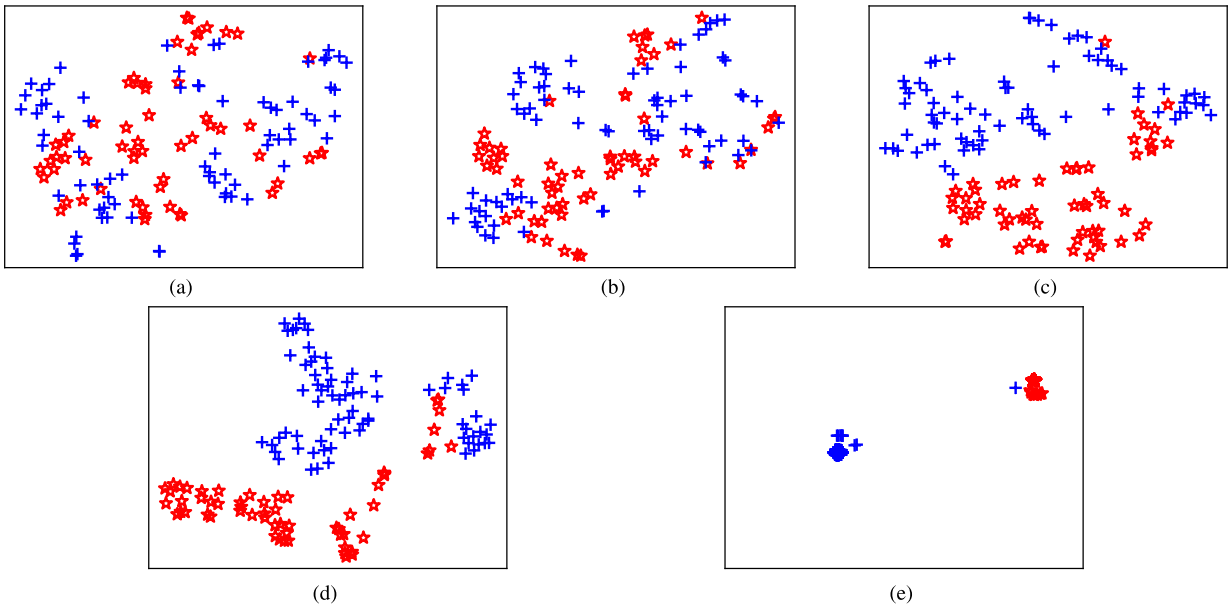

FIGURE 7. The Flatten Layer visualization using t-SNE for: (a) VGG16, (b) VGG19, (c) ResNet50, (d) EfficientNetB4, and (e) LeadNet.

C. COMPARISON WITH EXISTING MODELS

The Table 6 compares performance of the LEADNet and existing techniques based on the AFAVA dataset. Various EEG-based automatic Alzheimer's disease detection models have been reviewed earlier in Section I. However, Table 5 compares the performance of the existing models against the

TABLE 6. Comparison of LEADNet and existing techniques using the AFAVA dataset.

Paper	Method	CA	SNS	SPC
Abasolo *et al.* [12]	SpEn and SampEn	77.27	90.91	63.64
Abasolo *et al.* [15]	ApEn and AMI	90.91	100	81.82
Azami *et al.* [17]	GMSEn	72.73	75.86	80.68
Simons *et al.* [18]	FuzzyEn	86.36	81.82	90.91
Simons *et al.* [32]	Q-SpEn	77.27	79.19	77.97
Simons *et al.* [33]	LZC distance	77.27	72.73	81.82
Abasolo *et al.* [35]	DMA	81.82	90.91	72.73
Escudero *et al.* [31]	MSEn	90.91	90.91	90.91
Abasolo *et al.* [25]	DFA - LDA	95.45	90.91	100
Present work	**LEADNet Model**	**99.24**	**100**	**98.18**

developed LEADNet in terms of CA, SNS, and SPC. As per Table 6, the developed LEADNet attained higher CA, SNS, and SPC results than the existing models.

Abásolo et al. [25] improved accuracy to 95.45% using detrended fluctuation analysis (DFA), AMI, detrended moving average. However, these models are limited due to the time-varying and parametric entropy-based methods [12], [31]. Simon et al. [32] explored various techniques such as quadratic SpEn, generalized MSE, distance-based LZC [33], and FuEn [18] achieving an AD detection accuracy of 86.36% using the Mann-Whitney U-test and Lilliefors test. Puri et al. [34] investigated the wavelet packet subband-based features with traditional machine learning models. However, it reached a 95% classification rate. The performance of this method is dynamic [19]. In general, methods in Table 5 utilize duration-dependent features, failing to focus on frequency domain information. Some directions for future work are:

- Increasing the size and diversity of the population included in the dataset could improve the suggested CNN model's generalizability. Its performance can be enhanced by including data from various demographic groups, ethnicities, and disease stages.
- Investigating transfer learning techniques could help to improve the CNN model's performance on this job by fine-tuning it specifically for AD detection.
- Creating tools to analyze and visualize CNN's decision-making process can improve the model's reliability and transparency, making it more enticing for clinical use.

IV. CONCLUSION

These days, early and reliable AD detection is the primary concern. An effective AD detection method using a low-complexity convolutional neural network, LEADNet, is presented. The proposed model generated disease-specific features using spatiotemporal EEG signals. It used two convolutional layers, one max-pooling layer, two fully-connected layers, and a softmax layer. With CA: 99.24% SNS:100%, SPC: 98.18%, and F-score: 99.35% over the testing subset, the LEADNet performed better than the other pre-trained and state-of-the-art models. Because of its reduced complexity compared to other models, it is an excellent option for real-world healthcare scenarios. This work has highlighted the shortcomings of hand-crafted methods based on features and current clinical tests for AD detection, highlighting the demand for more independent and reliable methods. In summary, this work has advanced the use of CNNs and EEG signals for the early identification of AD. Due to its good performance in AD detection, this model might have broader potential applications than AD; it may also be helpful in the diagnosis of other neurological conditions like epilepsy and sleep problems.

REFERENCES

[1] J. Jeong, "EEG dynamics in patients with Alzheimer's disease," *Clin. Neurophysiol.*, vol. 115, no. 7, pp. 1490–1505, Jul. 2004.

[2] Z. Breijyeh and R. Karaman, "Comprehensive review on Alzheimer's disease: Causes and treatment," *Molecules*, vol. 25, no. 24, p. 5789, Dec. 2020.

[3] S. report, "Alzheimer's disease facts and figures," *Alzheimer's Dementia*, vol. 18, no. 4, pp. 700–789, 2022.

[4] I. A. Fouad and F. El-Zahraa M. Labib, "Identification of Alzheimer's disease from central lobe EEG signals utilizing machine learning and residual neural network," *Biomed. Signal Process. Control*, vol. 86, Sep. 2023, Art. no. 105266.

[5] A. Modir, S. Shamekhi, and P. Ghaderyan, "A systematic review and methodological analysis of EEG-based biomarkers of Alzheimer's disease," *Measurement*, vol. 220, Oct. 2023, Art. no. 113274.

[6] P. Ghorbanian, D. M. Devilbiss, T. Hess, A. Bernstein, A. J. Simon, and H. Ashrafiuon, "Exploration of EEG features of Alzheimer's disease using continuous wavelet transform," *Med. Biol. Eng. Comput.*, vol. 53, no. 9, pp. 843–855, Sep. 2015.

[7] D. Puri, S. Nalbalwar, A. Nandgaonkar, and A. Wagh, "Alzheimer's disease detection from optimal electroencephalogram channels and tunable Q-wavelet transform," *Indonesian J. Electr. Eng. Comput. Sci.*, vol. 25, pp. 1420–1428, Mar. 2022.

[8] B. Jiao, R. Li, H. Zhou, K. Qing, H. Liu, H. Pan, Y. Lei, W. Fu, X. Wang, and X. Xiao, "Neural biomarker diagnosis and prediction to mild cognitive impairment and Alzheimer's disease using EEG technology," *Alzheimer's Res. Therapy*, vol. 15, no. 1, pp. 1–14, 2023.

[9] S. Yuan, J. Liu, J. Shang, X. Kong, Q. Yuan, and Z. Ma, "The Earth mover's distance and Bayesian linear discriminant analysis for epileptic seizure detection in scalp EEG," *Biomed. Eng. Lett.*, vol. 8, no. 4, pp. 373–382, Nov. 2018.

[10] P. L. Giudice, N. Mammone, F. C. Morabito, R. G. Pizzimenti, D. Ursino, and L. Virgili, "Leveraging network analysis to support experts in their analyses of subjects with MCI and AD," *Med. Biol. Eng. Comput.*, vol. 57, no. 9, pp. 1961–1983, Sep. 2019.

[11] D. V. Puri, J. P. Gawande, J. L. Rajput, and S. L. Nalbalwar, "A novel optimal wavelet filter banks for automated diagnosis of Alzheimer's disease and mild cognitive impairment using electroencephalogram signals," *Decis. Anal. J.*, vol. 9, Dec. 2023, Art. no. 100336.

[12] D. Abásolo, R. Hornero, P. Espino, D. Álvarez, and J. Poza, "Entropy analysis of the EEG background activity in Alzheimer's disease patients," *Physiolog. Meas.*, vol. 27, no. 3, pp. 241–253, Jan. 2006.

[13] D. Puri, R. Chudiwal, J. Rajput, S. Nalbalwar, A. Nandgaonkar, and A. Wagh, "Detection of alcoholism from EEG signals using spectral and Tsallis entropy with SVM," in *Proc. Int. Conf. Commun. Inf. Comput. Technol. (ICCICT)*, Jun. 2021, pp. 1–5.

[14] D. V. Puri, P. H. Kachare, and S. L. Nalbalwar, "Metaheuristic optimized time–frequency features for enhancing Alzheimer's disease identification," *Biomed. Signal Process. Control*, vol. 94, Aug. 2024, Art. no. 106244.

[15] D. Abásolo, J. Escudero, R. Hornero, C. Gómez, and P. Espino, "Approximate entropy and auto mutual information analysis of the electroencephalogram in Alzheimer's disease patients," *Med. Biol. Eng. Comput.*, vol. 46, pp. 1019–1028, Oct. 2008.

[16] D. Puri, S. Nalbalwar, A. Nandgaonkar, and A. Wagh, "EEG-based diagnosis of Alzheimer's disease using Kolmogorov complexity," in *Applied Information Processing Systems*. Singapore: Springer, 2022, pp. 157–165.

[17] H. Azami, D. Abásolo, S. Simons, and J. Escudero, "Univariate and multivariate generalized multiscale entropy to characterise EEG signals in Alzheimer's disease," *Entropy*, vol. 19, no. 1, pp. 1–17, 2017.
[18] S. Simons, P. Espino, and D. Abásolo, "Fuzzy entropy analysis of the electroencephalogram in patients with Alzheimer's disease: Is the method superior to sample entropy?" *Entropy*, vol. 20, no. 1, p. 21, Jan. 2018.
[19] D. Puri, S. Nalbalwar, A. Nandgaonkar, and A. Wagh, "Alzheimer's disease detection with optimal EEG channel selection using wavelet transform," in *Proc. Int. Conf. Decis. Aid Sci. Appl. (DASA)*, Mar. 2022, pp. 443–448.
[20] A. Zandbagleh, A. Miltiadous, S. Sanei, and H. Azami, "Beta-to-theta entropy ratio of EEG in aging, frontotemporal dementia, and Alzheimer's dementia," *Amer. J. Geriatric Psychiatry*, Jul. 2024. [Online]. Available: https://www.sciencedirect.com/science/article/pii/S1064748124003804
[21] D. Abásolo, R. Hornero, C. Gómez, M. García, and M. López, "Analysis of EEG background activity in Alzheimer's disease patients with Lempel–Ziv complexity and central tendency measure," *Med. Eng. Phys.*, vol. 28, no. 4, pp. 315–322, May 2006.
[22] J. Dauwels, F. Vialatte, T. Musha, and A. Cichocki, "A comparative study of synchrony measures for the early diagnosis of Alzheimer's disease based on EEG," *NeuroImage*, vol. 49, no. 1, pp. 668–693, Jan. 2010.
[23] A. Cataldo, S. Criscuolo, E. De Benedetto, A. Masciullo, M. Pesola, J. Picone, and R. Schiavoni, "EEG complexity-based algorithm using multiscale fuzzy entropy: Towards a detection of Alzheimer's disease," *Measurement*, vol. 225, Feb. 2024, Art. no. 114040.
[24] S. Criscuolo, A. Cataldo, E. De Benedetto, A. Masciullo, M. Pesola, and R. Schiavoni, "Entropy and coherence features in EEG-based classification for Alzheimer's disease detection," in *Proc. IEEE Int. Instrum. Meas. Technol. Conf. (I2MTC)*, May 2024, pp. 1–6.
[25] D. Abasolo, R. Hornero, J. Escudero, and P. Espino, "A study on the possible usefulness of detrended fluctuation analysis of the electroencephalogram background activity in Alzheimer's disease," *IEEE Trans. Biomed. Eng.*, vol. 55, no. 9, pp. 2171–2179, Sep. 2008.
[26] K. Smith, D. Abásolo, and J. Escudero, "Accounting for the complex hierarchical topology of EEG phase-based functional connectivity in network Binarisation," *PLoS ONE*, vol. 12, no. 10, Oct. 2017, Art. no. e0186164.
[27] I. Al-Shourbaji, P. H. Kachare, L. Abualigah, M. E. Abdelhag, B. Elnaim, A. M. Anter, and A. H. Gandomi, "A deep batch normalized convolution approach for improving COVID-19 detection from chest X-ray images," *Pathogens*, vol. 12, no. 1, p. 17, Dec. 2022.
[28] A. Tharwat, "Classification assessment methods," *Appl. Comput. Informat.*, vol. 17, no. 1, pp. 168–192, Jan. 2021.
[29] A. Kamble, P. Ghare, and V. Kumar, *Classifying Phonological Categories Imagined Words From EEG Signal*. Boca Raton, FL, USA: CRC Press, May 2021, pp. 93–121.
[30] P. Kachare, D. Puri, S. B. Sangle, I. Al-Shourbaji, A. Jabbari, R. Kirner, A. Alameen, H. Migdady, and L. Abualigah, "LCADNet: A novel light CNN architecture for EEG-based Alzheimer disease detection," *Phys. Eng. Sci. Med.*, vol. 47, pp. 1–14, Jun. 2024.
[31] J. Escudero, D. Abásolo, R. Hornero, P. Espino, and M. López, "Analysis of electroencephalograms in Alzheimer's disease patients with multiscale entropy," *Physiolog. Meas.*, vol. 27, no. 11, pp. 1091–1106, Sep. 2006.
[32] S. Simons, D. Abasolo, and J. Escudero, "Classification of Alzheimer's disease from quadratic sample entropy of electroencephalogram," *Healthcare Technol. Lett.*, vol. 2, no. 3, pp. 70–73, Jun. 2015.
[33] S. Simons and D. Abásolo, "Distance-based Lempel–Ziv complexity for the analysis of electroencephalograms in patients with Alzheimer's disease," *Entropy*, vol. 19, no. 3, p. 129, Mar. 2017.
[34] D. V. Puri, S. L. Nalbalwar, and P. P. Ingle, "EEG-based systematic explainable Alzheimer's disease and mild cognitive impairment identification using novel rational dyadic biorthogonal wavelet filter banks," *Circuits, Syst., Signal Process.*, vol. 43, no. 3, pp. 1792–1822, Mar. 2024.
[35] D. Abasolo, R. Hornero, C. Gomez, J. Escudero, and P. Espino, "Electroencephalogram background activity characterization with detrended moving average in Alzheimer's disease patients," in *Proc. IEEE Int. Symp. Intell. Signal Process.*, Aug. 2009, pp. 211–215.

DIGAMBAR V. PURI received the B.Tech. degree in electronics and telecommunication engineering from Dr. Babasaheb Ambedkar Technological University, Lonere, in 2012, the M.Tech. degree in electronics and telecommunication engineering from Veermata Jijabai Technological Institute Matunga, University of Mumbai, India, in 2015, and the Ph.D. degree in electronics and telecommunication engineering from Dr. Babasaheb Ambedkar Technological University, in 2023. Currently, he is an Assistant Professor of computer science and engineering with Ramrao Adik Institute of Technology, Nerul, Navi Mumbai. He has published articles in various high-impact factor, peer-reviewed journals and conferences. He has written a book on *Signals and Systems* in Nirali publications. His research interests include biomedical signal processing, pattern recognition, machine learning, data analysis, and image processing. He serves as a reviewer in various journals in Elsevier and Springer.

PRAMOD H. KACHARE received the B.E. degree in electronics and telecommunication engineering from the Don Bosco Institute of Technology, University of Mumbai, India, in 2012, and the M.Tech. degree in electronics and telecommunication engineering from the Veermata Jijabai Technological Institute Matunga, University of Mumbai, in 2015. He joined the Ramrao Adik Institute of Technology, Navi Mumbai, India, in 2015, as an Assistant Professor of computer science and engineering. He has published articles in several peer-reviewed journals and conferences. His research interests include speech and signal processing, machine learning, and metaheuristic optimization. He serves as a reviewer for various international journals and conferences.

SANDEEP B. SANGLE received the B.E. degree in electronics engineering from Pune University, in 2012, and the M.E. and Ph.D. degrees in electronics and telecommunication engineering from the Ramrao Adik Institute of Technology, University of Navi Mumbai, Navi Mumbai, India, in 2016 and 2023, respectively. He joined computer science and engineering with the Ramrao Adik Institute of Technology, in 2014, where he is an Assistant Professor. He has published articles in various high-impact, peer-reviewed journals and conferences. He serves as a reviewer for multiple international conferences. His research interests include speech processing, biomedical signal processing, statistical methods, machine learning, and deep learning.

RAIMUND KIRNER received the Ph.D. degree from TU Vienna, in 2003. He holds a position as a Reader of cyber-physical systems with the University of Hertfordshire. He has been a Principal Investigator of numerous national and European research projects. He has published more than 100 refereed journal and conference papers and received two patents. His research interests include intelligent and secure cyber-physical systems. He is a member of the IFIP Working Group 10.2 (Embedded Systems).

ABDOH JABBARI received the B.S. degree in network engineering from Johnson and Wales University, RI, USA, the M.S. degree in computer information and network security from DePaul University, Chicago, IL, USA, and the Ph.D. degree in telecommunications and computer networking from the University of Missouri–Kansas City. He is currently an Associate Professor with the Department of Electrical and Electronics Engineering, Jazan University. His research interests include the IoT, blockchain, SDN, smart applications, machine learning, and sensor enhancements.

IBRAHIM AL-SHOURBAJI received the Ph.D. degree from the University of Hertfordshire, U.K. He holds an associate position with the Department of Electrical and Electronics Engineering, Jazan University, Saudi Arabia. He has published several journal papers, conferences, and books. His main research interests include computational intelligence, metaheuristic algorithms, signal processing, deep learning, robotics, and optimization. He serves as a reviewer for many prestigious journals in Elsevier, Springer, and IEEE.

MOHAMMED ABDALRAHEEM received the B.Sc. degree in computer science from the International University of Africa, Sudan, the master's degree in computer science and artificial intelligence track from Sudan University of Science and Technologies, and the Ph.D. degree in computer science from Alneelain University. He is currently an Assistant Professor with the Department of Computer Science, Jazan University. He has published many refeed and conference papers. He is a member of the Computer Professionals Society in Sudan.

ABDALLA ALAMEEN received the M.Sc. degree in information technology and the Ph.D. degree in computer science from Al Neelain University, Sudan, in 2010 and 2013, respectively. He is a Distinguished Professor of computer science with the College of Engineering, Prince Sattam Bin Abdulaziz University, Wadi ad-Dawasir, Saudi Arabia. His extensive academic career includes positions ranging from a Lecturer to a Full Professor, with significant contributions to teaching and research. He has spearheaded pioneering research in interdisciplinary programs, focusing on information and network security, cloud computing, and emerging digital technologies. He has published numerous papers in esteemed journals and presented them at various conferences and workshops. His research activities primarily focus on several areas within computer science, including machine learning, optimization algorithms, cybersecurity, and the IoT. He is also a member of several professional organizations, including the International Association of Engineers (IAENG) and the Institute for Computer Sciences, Social Informatics, and Telecommunications Engineering (ICST).